Journal of Sound and Vibration (1999) **225**(2), 375–389
Article No. jsvi.1999.2283, available online at http://www.idealibrary.com on IDEAL®

NON-LINEAR VIBRATIONS OF A DISCRETE-CONTINUOUS TORSIONAL SYSTEM WITH NON-LINEARITIES HAVING CHARACTERISTIC OF A SOFT TYPE

A. PIELORZ

Institute of Fundamental Technological Research, Swiętokrzyska 21, 00–049 *Warsaw, Poland*

(*Received* 11 *November* 1998, *and in final form* 19 *April* 1999)

In this paper a non-linear discrete-continuous model of a multi-mass system torsionally deformed with a local non-linearity is investigated. It is assumed that the characteristic of the local non-linearity is of a soft type. Four non-linear functions describing this characteristic are proposed. In the discussion, the approach utilizing the wave solution of the equations of motion is used, similarly as for the case of a hard characteristic in reference [1]. The numerical analysis focuses on the investigation of the effect of the local non-linearity with a soft characteristic for two-mass and three-mass torsional systems on amplitude–frequency curves in selected cross-sections of the considered systems.

1. INTRODUCTION

The paper is concerned with the non-linear dynamics of discrete-continuous models of torsional mechanical systems. These systems consist of shafts with a circular cross-section connected by means of rigid bodies. The displacements of shaft cross-sections are described by means of the classical wave equation, as in reference [1]. In many drive systems gears, clutches, etc., having non-linear characteristics can occur [2]. Such non-linearities in mechanical systems have a local character, which means that in discrete-continuous models they can be taken into account in appropriate cross-sections. The presence of local non-linearities in the mechanical system can have important consequences for its overall dynamic behaviour. Some effects of the local non-linearities in discrete-continuous systems have been already shown e.g., in references [1, 3].

Reference [1] is concerned with the dynamic analysis of a non-linear discrete-continuous torsional system with a non-linearity represented by a spring having a hard characteristic of the Duffing type. Below, a similar discrete-continuous model of the mechanical system torsionally deformed is studied. However, the non-linear spring has the characteristic of a soft type. The moment of the non-linear spring is described by four non-linear functions: (1) a polynomial of third degree, (2) a sinusoidal function, (3) a hyperbolic tangent function, and (4) an

0022-460X/99/320375 + 15 $30.00/0

exponential function. Such types of functions are justified by numerous experimental studies [4]. The polynomial function can be used in the case of the spring having soft as well as hard characteristics, while the remaining ones only in soft characteristics. The introduction of three other functions for non-linear moments not only expands the discussion on local non-linearities but also enables one to avoid such effect as the escape which may appear in numerical solutions for non-linear models. Some examples of this escape are shown in reference [5] for discrete models.

The considerations are carried out by means of the method using the wave solution of the equations of motion which enables one to determine displacements in arbitrary cross-sections of shafts. Solutions can be obtained in steady as well as in transient states. In numerical calculations the effect of various non-dimensional parameters on amplitude–frequency curves for angular displacements and non-linear moments for a two-mass and a three-mass system is investigated.

The method applied in the paper was verified experimentally. The test-rig used for torsional analysis is a transmission system driven by an electric servo-motor. Its detailed description can be found in reference [6]. Theoretical considerations for the appropriate discrete-continuous model are presented in reference [7]. The comparable studies given in reference [7] show a very good agreement between the experimental data and the numerical solutions.

2. ASSUMPTIONS, MOMENTS FOR THE NON-LINEAR SPRING

Consider the discrete-continuous model of a system which consists of a suitable number of rigid bodies connected by shafts, Figure 1. The shafts only deform in torsion-like manner and their central axis, together with elements settled on them, coincide with the main axis of the torsional system. It is assumed that the x-axis is parallel to the main axis of the system, and its origin coincides with the location of the left end first shaft in an undisturbed state at time instant $t = 0$.

The ith shaft, $i = 1, 2, \ldots, N$, Figure 1, is characterized by the length l_i, density ρ, shear modulus G and polar moment of inertia I_{0i}. The ith rigid body of the model is characterized by mass moment of inertia J_i.

In the considered discrete-continuous model a single local non-linearity is taken into account by means of a non-linear discrete spring. This element is located in the cross-section where the rigid body J_i is fixed. It can represent, for example, mechanical properties of various elements, such as clutches and gears, having a non-linear characteristic.

The moment of a non-linear spring can be generally described by an arbitrary non-linear function [2]. In the discussion of the dynamics of non-linear discrete systems the polynomial of the third degree is exploited most widely for the description of the considered non-linearities [8, 9]. In the present paper, it is used in the case of the discrete-continuous torsional system. Analogous to non-linearities in discrete systems, the moment for the non-linear spring with a symmetric characteristic could be described by the following function:

$$M_{sp}(t) = k_1\theta_1(x, t) + k_3\theta_1^3(x, t) \quad \text{for } x = 0, \tag{1}$$

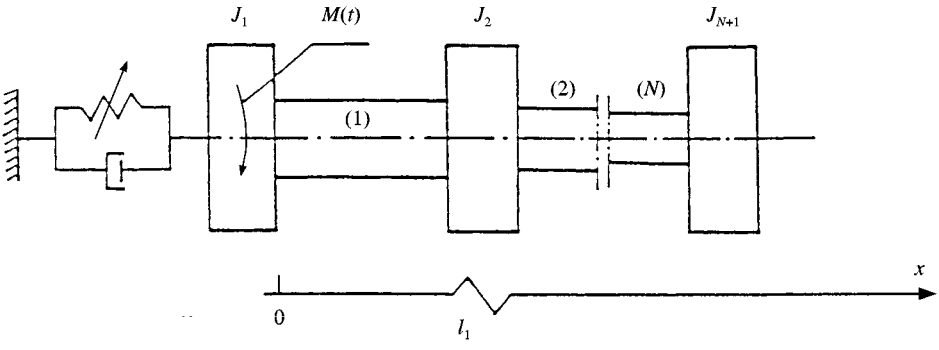

Figure 1. The non-linear discrete-continuous model of a torsional system.

where $\theta_i(x, t)$ is an angular displacement of the ith shaft and k_1 and k_3 represent linear and non-linear terms in equation (1) respectively. The polynomial (1) includes the soft characteristic for $k_3 < 0$, the linear case for $k_3 = 0$ and the hard characteristic for $k_3 > 0$.

In many non-linear discrete systems, where this function with $k_3 < 0$ (the soft characteristic) is used, such phenomena as escapes may occur [5]. In order to try to avoid the divergence of numerical solutions to infinity in the case of the soft characteristic, apart from the polynomial function (1) with $k_3 < 0$ the following three functions are proposed for the description of moments for the non-linear spring applied in the cross-section $x = 0$

$$M_{sp}(t) = A \sin(B\theta_1), \tag{2}$$

$$M_{sp}(t) = A \tanh(B\theta_1), \tag{3}$$

$$M_{sp}(t) = \begin{cases} A(-1 + \exp(B\theta_1)) & \text{for } \theta_1 \leqslant 0, \\ A(1 - \exp(-B\theta_1)) & \text{for } \theta_1 \geqslant 0.' \end{cases} \tag{4}$$

The constants A and B are selected in such a way that the expansions in series of functions (2)–(4) give the same linear case and that the polynomial function (1) and functions (2)–(4) have maximum values close to each other, and

$$AB = k_1, \quad AB^3 = -6k_3. \tag{5}$$

In the discussed non-linear model an external loading $M(t)$ can be applied to an arbitrary rigid body. In the present paper it is assumed that only the rigid body J_1 is loaded by the external loading $M(t)$. Damping in the system is taken into account by an equivalent external and internal damping applied in selected cross-sections. It is expressed by the following moments:

$$M_{di}(t) = d_i \theta_{i,t}(x, t) \quad \text{and} \quad M_{Di}(t) = GI_{0i} D_i \theta_{i,xt}(x, t), \tag{6}$$

where d_i and D_i are the coefficients of the equivalent external and internal damping, respectively, and the comma denotes partial differentiation. Moreover, it is assumed that displacements and velocities of shaft cross-sections are equal to zero at time instant $t = 0$.

3. GOVERNING EQUATIONS

Under the above assumptions, the determination of angular displacements $\theta_i(x, t)$ of the shaft cross-sections reduces to the solution of classical wave equations

$$\theta_{i,tt} - c^2\theta_{i,xx} = 0, \quad i = 1, 2, \ldots, N \tag{7}$$

with zero initial conditions

$$\theta_i(x, 0) = \theta_{i,t}(x, 0) = 0, \quad i = 1, 2, \ldots, N, \tag{8}$$

and with the following non-linear boundary conditions:

$$\begin{gathered}
M(t) - J_1\theta_{1,tt} + \mathrm{GI}_{01}(D_1\theta_{1,xt} + \theta_{1,x}) - d_1\theta_{1,t} - M_{sp}(t) = 0 \quad \text{for } x = 0, \\
\theta_i(x, t) = \theta_{i+1}(x, t) \quad \text{for } x = \sum_{k=1}^{i} l_k, \quad i = 1, 2, \ldots, N-1 \\
- J_{i+1}\theta_{i,tt} - \mathrm{GI}_{0i}(D_i\theta_{i,xt} + \theta_{i,x}) + \mathrm{GI}_{0,i+1}(D_{i+1}\theta_{i+1,xt} + \theta_{i+1,x}) \\
- d_{i+1}\theta_{i,t} = 0 \quad \text{for } x = \sum_{k=1}^{i} l_k, \quad i = 1, 2, \ldots, N-1, \\
- J_{N+1}\theta_{N,tt} - \mathrm{GI}_{0N}(D_N\theta_{N,xt} + \theta_{N,x}) - d_{N+1}\theta_{N,t} = 0 \quad \text{for } x = \sum_{k=1}^{N} l_k,
\end{gathered} \tag{9}$$

where $c^2 = G/\rho$.

Upon the introduction of the following non-dimensional quantities:

$$\begin{gathered}
\bar{x} = x/l_1, \quad \bar{t} = ct/l_1, \quad \bar{\theta}_i = \theta_i/\theta_0, \quad \bar{d}_i = d_i l_1/(J_1 c), \quad \bar{D}_i = D_i c/l_1, \\
\bar{k}_1 = k_1 l_1^2/(J_1 c^2), \quad \bar{k}_3 = k_3\theta_0^2 l_1^2/(J_1 c^2), \quad K_r = I_{01}\rho l_1/J_1, \quad E_i = J_1/J_i, \\
\bar{M} = M l_1^2/(J_1 c^2\theta_0), \quad \bar{M}_{sp} = M_{sp} l_1^2/(J_1 c^2\theta_0), \quad \bar{l}_i = l_i/l_1, \quad B_i = I_{0i}/I_{01},
\end{gathered} \tag{10}$$

relations (7)–(9) take the form

$$\theta_{i,tt} - \theta_{i,xx} = 0, \quad i = 1, 2, \ldots, N, \tag{11}$$

$$\theta_i(x, 0) = \theta_{i,t}(x, 0) = 0, \quad i = 1, 2, \ldots, N, \tag{12}$$

$$\begin{gathered}
M(t) - \theta_{1,tt} + K_r(D_1\theta_{1,xt} + \theta_{1,x}) - d_1\theta_{1,t} - M_{sp}(t) = 0 \quad \text{for } x = 0, \\
\theta_i(x, t) = \theta_{i+1}(x, t) \quad \text{for } x = \sum_{k=1}^{i} l_k, \quad i = 1, 2, \ldots, N-1 \\
- \theta_{i,tt} - K_r B_i E_{i+1}(D_i\theta_{i,xt} + \theta_{i,x}) + K_r B_{i+1} E_{i+1}(D_{i+1}\theta_{i+1,xt} + \theta_{i+1,x}) \\
- E_{i+1} d_{i+1}\theta_{i,t} = 0 \quad \text{for } x = \sum_{k=1}^{i} l_k, \quad i = 1, 2, \ldots, N-1 \\
- \theta_{N,tt} - K_r B_N E_{N+1}(D_N\theta_{N,xt} + \theta_{N,x}) - E_{N+1} d_{N+1}\theta_{N,t} = 0 \quad \text{for } x = \sum_{k=1}^{N} l_k,
\end{gathered} \tag{13}$$

where θ_0 is a fixed angular displacement, and the bars denoting non-dimensional quantities are omitted for convenience.

The solutions of equations (11) similar to reference [1] are sought in the form

$$\theta_i(x,t) = f_i(t-x) + g_i\left(t + x - 2\sum_{k=1}^{i-1} l_k\right), \quad i = 1,2,\ldots,N, \tag{14}$$

where the functions f_i and g_i represent waves caused by the external loading $M(t)$ propagating in the ith shaft in a direction consistent and opposite to x-axis, correspondingly. The functions f_i and g_i are continuous and equal to zero for negative arguments.

Substituting solution (14) in the boundary conditions (13) and denoting the largest argument in each boundary condition separately by z, we obtain the following set of ordinary differential equations for unknown functions f_i and g_i

$$\begin{aligned}
&r_{N+1,1}g_N''(z) + r_{N+1,2}g_N'(z) = r_{N+1,3}f_N''(z-2l_N) + r_{N+1,4}f_N'(z-2l_N),\\
&g_i(z) = f_{i+1}(z-2l_i) + g_{i+1}(z-2l_i) - f_i(z-2l_i), \quad i = 1,2,\ldots,N-1,\\
&r_{11}f_1''(z) = M(z) + r_{12}g_1''(z) + r_{13}f_1'(z) + r_{14}g_1'(z) - M_{sp}(z),\\
&r_{i1}f_i''(z) + r_{i2}f_i'(z) = r_{i3}g_i''(z) + r_{i4}g_i'(z) + r_{i5}f_{i-1}''(z) + r_{i6}f_{i-1}'(z), \quad i = 2,3,\ldots,N,
\end{aligned} \tag{15}$$

where

$$\begin{aligned}
&r_{11} = K_rD_1 + 1, \quad r_{12} = K_rD_1 - 1, \quad r_{13} = -K_r - d_1, \quad r_{14} = K_r - d_1,\\
&r_{i1} = K_rE_i(B_iD_i + B_{i-1}D_{i-1}) + 1, \quad r_{12} = E_i[K_r(B_i + B_{i-1}) + d_i],\\
&r_{i3} = K_rE_i(B_iD_i - B_{i-1}D_{i-1}) - 1, \quad r_{i4} = E_i[K_r(B_i - B_{i-1}) - d_i],\\
&r_{i5} = 2K_rB_{i-1}E_iD_{i-1}, \quad r_{i6} = 2K_rB_{i-1}E_i, \quad i = 2,3,\ldots,N\\
&r_{N+1,1} = K_rB_NE_{N+1}D_N + 1, \quad r_{N+1,2} = E_{N+1}(K_rB_N + d_{N+1}),\\
&r_{N+1,3} = K_rB_NE_{N+1}D_N - 1, \quad r_{N+1,4} = E_{N+1}(K_rB_N - d_{N+1}).
\end{aligned} \tag{16}$$

Equations (15) are differential equations with a retarded argument. Solving them in a given succession in the successive intervals of the argument z, the right-hand sides of these equations are always known. The non-linear equation is solved numerically by means of the Runge–Kutta method, and the linear differential equations are solved using the method of finite differences. Having obtained from equation (15) the functions f_i and g_i and their derivatives one can determine displacements strains and velocities in an arbitrary cross-section of the shafts at an arbitrary time instant utilizing relations (14). Non-linear equations (15) can be solved only numerically while linear discrete-continuous systems could be treated numerically as well as analytically [1, 10].

4. NUMERICAL RESULTS

In numerical investigations amplitude–frequency curves for angular displacements and for the moment M_{sp} are determined for the two-mass and three-mass torsional systems. The local non-linearity in these systems has the characteristic of a soft type. Some comparable calculations are presented in reference [1] for the single-mass system in the case of a hard characteristic.

The external moment $M(t)$ appearing in equations (15), similar to reference [1], is assumed in the form

$$M(t) = M_0 \sin(pt), \tag{17}$$

where p is a non-dimensional loading frequency. We focus on the solution in steady states. It should be pointed out that the wave method enables one to perform numerical solutions in a transient and in a steady state. Solutions in in transient states for linear systems are presented in reference [10].

Non-linear effects in the considered system are caused directly by the non-linear moment $M_{sp}(t)$ occurring in the cross-section $x = 0$ described by functions (1)–(4). On the other hand, the non-linear effects are also connected with the amplitude M_0 of the external moment and with the external and internal damping. In the performed numerical analysis damping coefficients are assumed to be constant, equal to $d_i = D_i = 0{\cdot}1$.

The polynomial function (1) consists of the linear and non-linear terms represented by coefficients k_1 and k_3 respectively. In numerical calculations the coefficient k_1 is fixed, while k_3 can vary. If $k_3 < 0$ then we propose to use functions (2)–(4) also with coefficients A and B calculated from (5) for the given values of k_1 and k_3. One can notice that polynomial functions (1) for $k_3 < 0$ and the sinusoidal functions (2) have their extremes. They can be useful for the values of θ_1 between these extremes where functions (1) and (2) are ascending functions. No limits of such a type are noted for the hyperbolic function (3) and the exponential function (4).

Numerical results given below are exemplary. In reference [1] among others, the amplitude–frequency curves are determined in various shaft cross-sections. All diagrams in the present paper concern the cross-section $x = 0$ where the non-linear discrete element is taken into account. The discussion is focused on the effect of this non-linear element having the characteristic of a soft type on displacements in $x = 0$ and on the non-linear moment M_{sp}. Suitable numerical results were performed for the two-mass and three-mass torsional systems.

4.1. TWO-MASS TORSIONAL SYSTEM

Numerical calculations for the two-mass torsional system, according to results presented in reference [1], are performed using equations (15) with the following basic parameters

$$K_r = 0{\cdot}05, \quad k_1 = 0{\cdot}05, \quad N = 1, \quad d_i = D_i = 0{\cdot}1, \quad E_2 = 0{\cdot}8. \tag{18}$$

In Figure 2 amplitude–frequency curves for the angular displacement in the cross-section $x = 0$ are plotted out with $k_3 = -0{\cdot}005$, $M_0 = 0{\cdot}03$, $0{\cdot}1$, $0{\cdot}15$ and $p \leqslant 1{\cdot}5$ using four functions (1)–(4) for the description of the non-linear moment M_{sp}. The diagrams include two resonant regions ($\omega_1 = 0{\cdot}126$, $\omega_2 = 0{\cdot}351$). In further resonant regions effects of the local non-linearity were not observed. For $M_0 = 0{\cdot}03$ in the first resonant region the highest amplitudes are obtained for the function (4) and the smallest ones for the functions (1) and (2). The solution for all

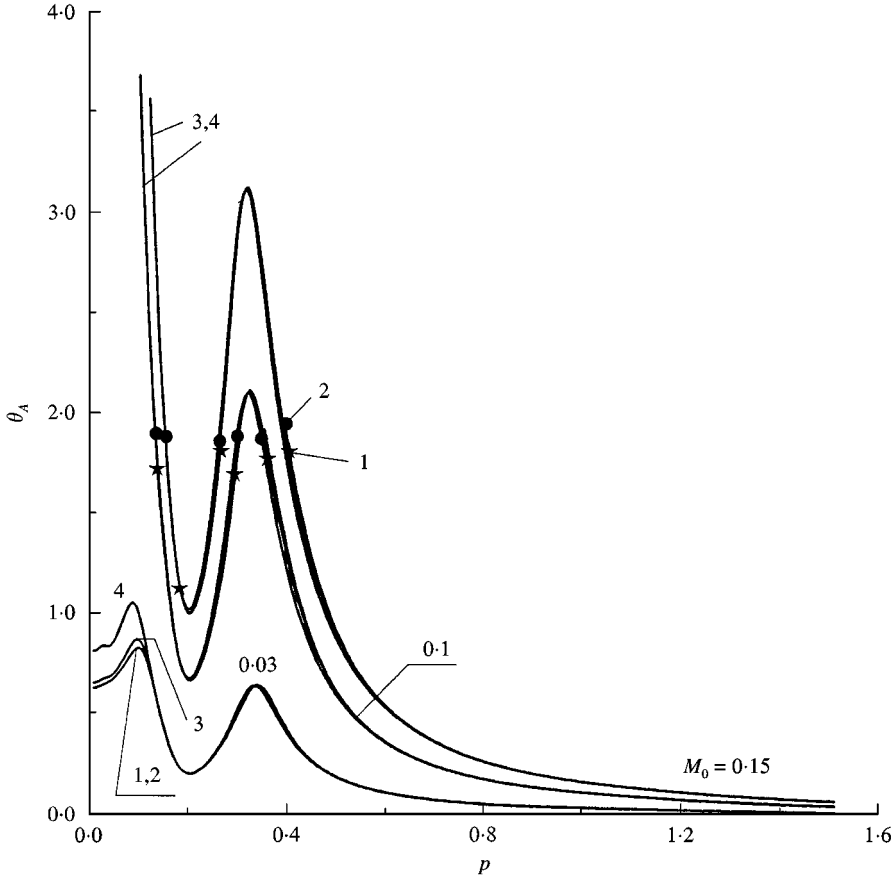

Figure 2. Amplitude–frequency curves for angular displacements in $x = 0$ for the two-mass system with $k_3 = -0{\cdot}005$, $M_0 = 0{\cdot}03$, $0{\cdot}1$, $0{\cdot}15$ with non-linear functions (1)–(4).

non-linear functions practically, give the same results in the second resonant region. When $M_0 = 0{\cdot}1$ and $0{\cdot}15$ the application of functions (3) and (4) results in practically identical amplitude–frequency curves. These curves also contain the curves obtained for functions (1) and (2) within their application ranges. The maximum displacement amplitudes for the solution being a harmonic function are marked by stars and spots for the polynomial function (1) and the sinusoidal function (2), respectively. These marks define the application ranges of the functions (1) and (2). They occur in the both considered resonant regions.

Amplitude–frequency diagrams for the non-linear moment M_{sp} are plotted out in Figure 3 for $k_3 = -0{\cdot}005$ and $M_0 = 0{\cdot}03$, $0{\cdot}15$. When $M_0 = 0{\cdot}03$, the maximal amplitudes are achieved with functions (1), (2) and the minimal ones with function (4) in the both considered resonant regions. The same conclusion is also valid for higher values of the amplitude of the external moment. The exceptions concern cases when the amplitude M_A achieves the maximums of the non-linear moment M_{sp} described by (1)–(4). Then the solutions with functions (3) and (4) from the 'plateau', while the solution with function (1) begins to diverge to infinity and the solution with function (2) is non-harmonic. Stars and spots on the

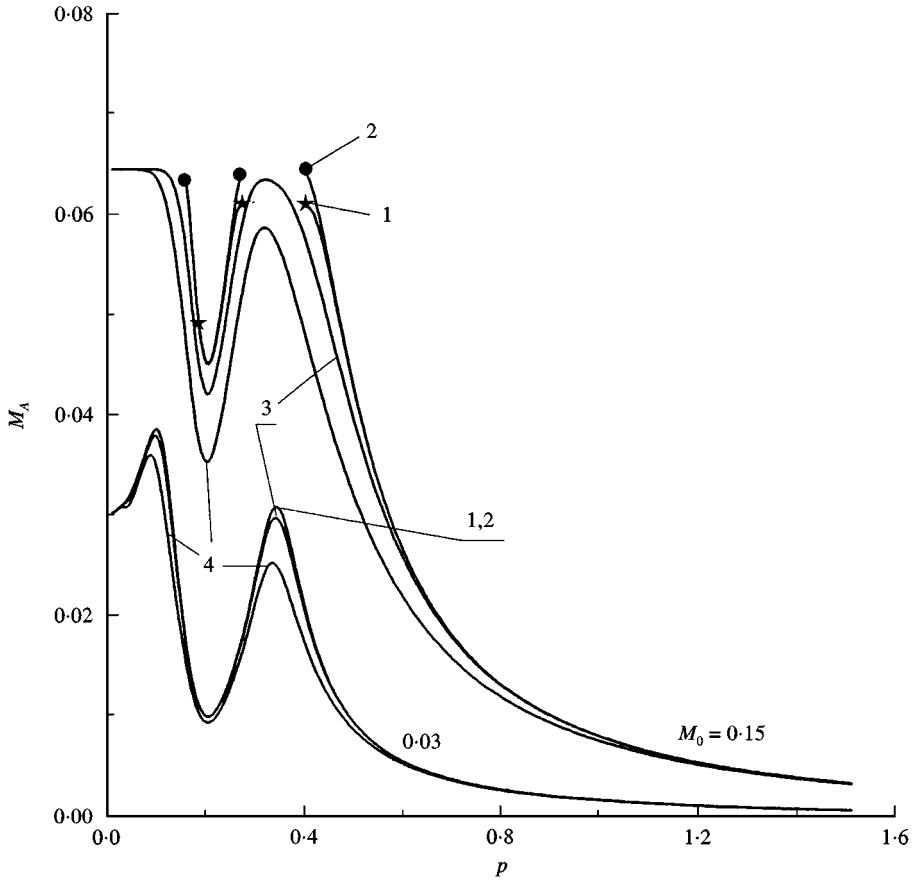

Figure 3. Amplitudes of the moment M_{sp} for the two-mass system for $k_3 = -0{\cdot}005$, $M_0 = 0{\cdot}03$, $0{\cdot}15$ with non-linear functions (1)–(4).

amplitude–frequency curves in Figure 3 indicate the maximum amplitudes M_A for the harmonic solutions determined when the polynomial function (1) and the sinusoidal function (2) are used.

The application ranges of functions (1) and (2) are investigated for $k_3 = -0{\cdot}0005$, $-0{\cdot}001$, $-0{\cdot}005$, $-0{\cdot}01$. Suitable curves are marked by dashed and continuous lines in Figure 4. These curves determine the amplitudes of the external moment (17) below which numerical solutions behave as harmonic functions with the period equal to the period of the external moment. The smallest values for M_0 are acceptable in the neighbourhood of the resonances. From Figure 4 it also follows that for the fixed k_3 the application ranges are slightly wider in the case of the sinusoidal function (2). It is connected with the fact that the function M_{sp} has higher maximum values when the sinusoidal function (2) is applied. Besides, there exists the interval of p where admissible values of M_0 increase in a linear manner when function (1) is assumed. This interval occurs between the first and the second resonances, Figure 4.

No restrictions similar to those connected with the application of the non-linear functions (1) and (2) have been found in the case of functions (3) and (4). Thus, the

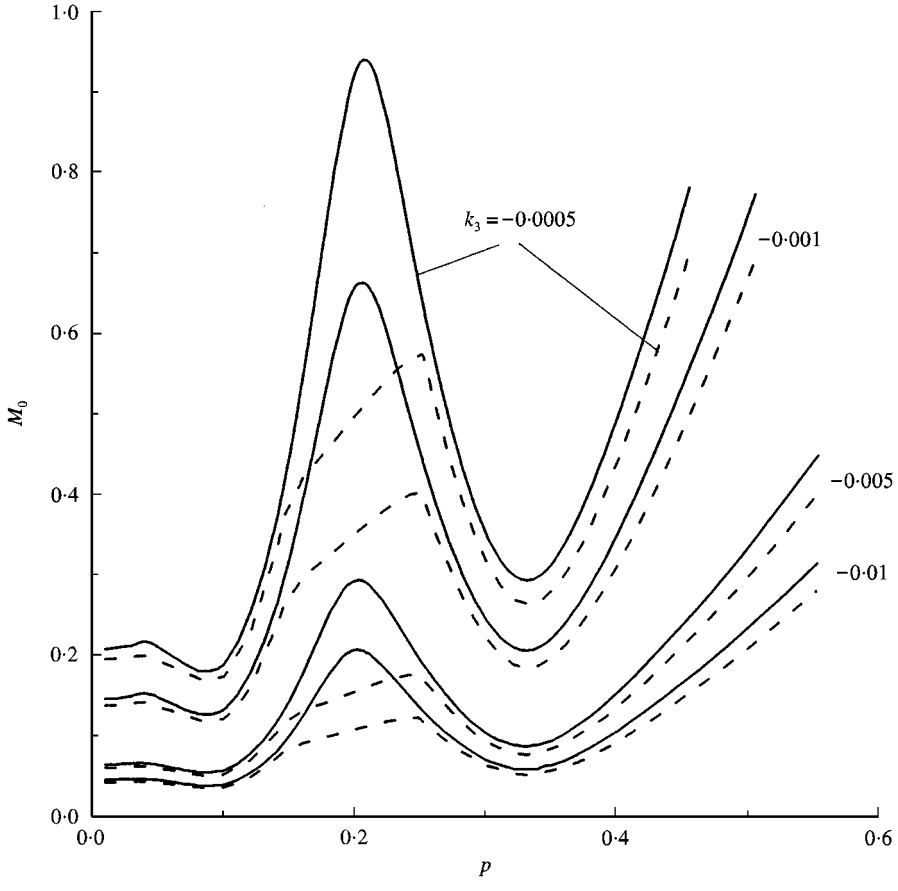

Figure 4. Application ranges of the sinusoidal function (continuous lines) and polynomial function (dashed lines) for the two-mass system with $k_3 = -0{\cdot}0005,\ -0{\cdot}001,\ -0{\cdot}005,\ -0{\cdot}01$.

non-linear functions (3) and (4) can be used in the discussion of the effect of various parameters on the dynamic behaviour of torsional systems. The solution with the both functions are similar. In Figure 5 the effect of the parameter k_3 on the amplitude of the angular displacements in $x = 0$ of the two-mass system is shown. For this purpose equations (15) are solved with the hyperbolic tangent function (3) for $k_3 = 0,\ -0{\cdot}0005,\ -0{\cdot}001,\ -0{\cdot}005,\ -0{\cdot}01$ and $M_0 = 0{\cdot}1$. From Figure 5 it follows that the maximal displacement amplitudes increase with the decrease of k_3 in the first resonant region while in the second resonant region they decrease with the decrease of k_3.

4.2. THREE-MASS TORSIONAL SYSTEM

Numerical calculations for the three-mass torsional system are performed using equations (15) with the following basic parameters [1],

$$K_r = 0{\cdot}05, \quad k_1 = 0{\cdot}05, \quad N = 2, \quad l_1 = l_2 = 1,$$
$$d_1 = D_i = 0{\cdot}1, \quad E_2 = E_3 = 0{\cdot}8, \quad B_2 = 1. \tag{19}$$

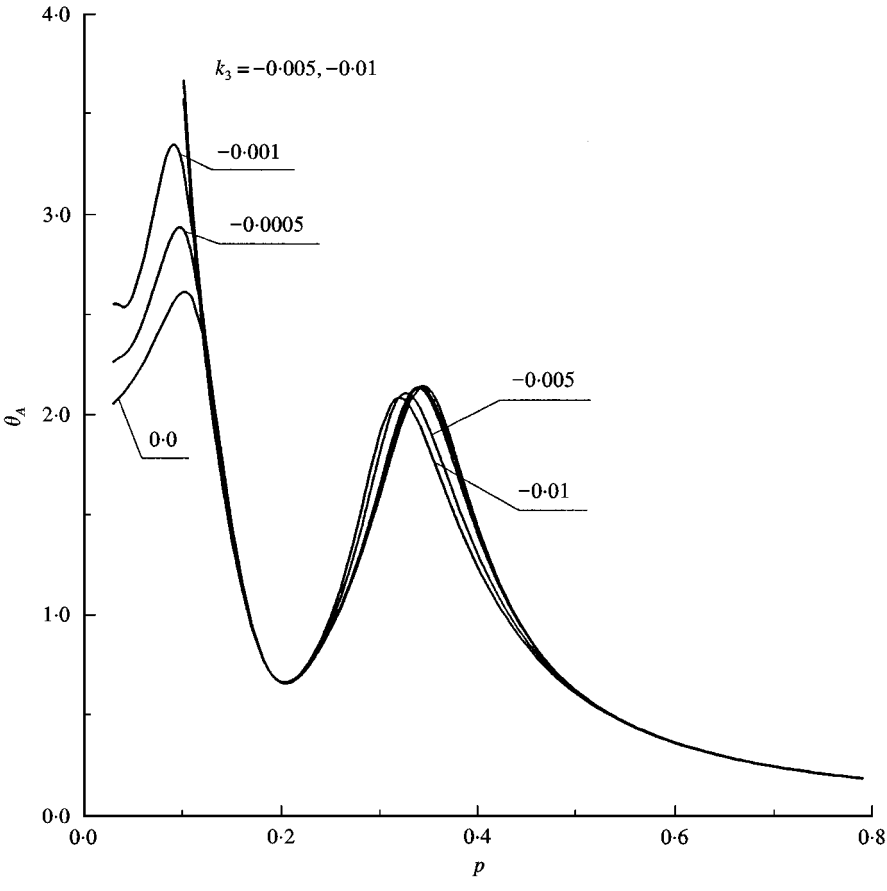

Figure 5. Effect of the parameter k_3 on displacement amplitudes for the two-mass system with $M_0 = 0{\cdot}1$, $k_3 = 0, \ -0{\cdot}0005, \ -0{\cdot}001, \ -0{\cdot}005, \ -0{\cdot}01$ for the hyperbolic tangent function.

In Figure 6 amplitude–frequency curves for the angular displacement in the cross-section $x = 0$ of the three-mass system are plotted out with $k_3 = -0{\cdot}005$, $M_0 = 0{\cdot}03, 0{\cdot}1, 0{\cdot}15$. Four functions (1)–(4) were used for the description of the non-linear moment M_{sp}. The diagrams include three resonant regions ($\omega_1 = 0{\cdot}089$, $\omega_2 = 0{\cdot}261$, $\omega_3 = 0{\cdot}376$). In further resonant regions, no non-linear effects were observed. For $M_0 = 0{\cdot}03$ in the first and the second resonant regions the highest amplitudes are obtained for function (4) and the smallest ones for functions (1) and (2). The solution for all non-linear functions give practically the same results in the third resonant region. When $M_0 = 0{\cdot}1$ and $0{\cdot}15$ the application of functions (3) and (4) results in practically identical amplitude–frequency curves apart from the resonances. These curves contain also the curves obtained for the functions (1) and (2) within their application ranges. Similarly, as in the case of the two-mass systems, the maximum displacement amplitudes for the harmonic solution are correspondingly marked by stars and spots for the polynomial function (1) and the sinusoidal function (2). Now, these marks defining the application ranges of functions (1) and (2) occur in the all three considered resonant regions.

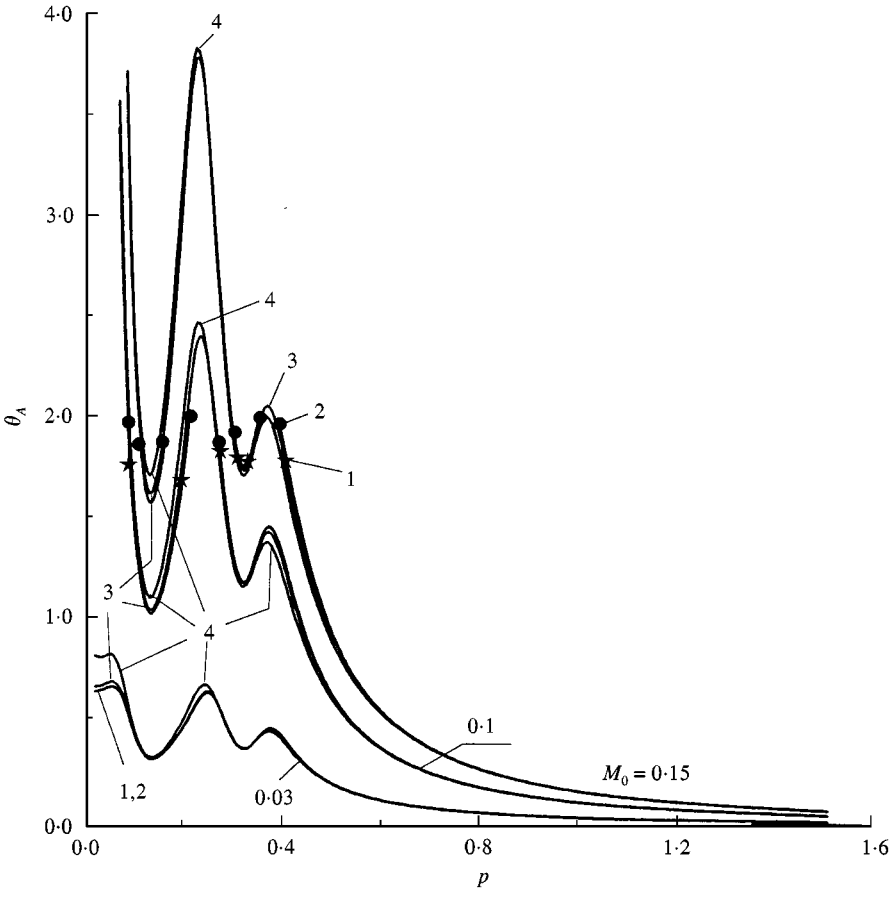

Figure 6. Amplitude–frequency curves for angular displacements in $x = 0$ for the three-mass system for $k_3 = -0{\cdot}005$, $M_0 = 0{\cdot}03$, $0{\cdot}1$, $0{\cdot}15$ with non-linear functions (1)–(4).

The amplitude–frequency diagrams for the moment M_{sp} according to functions (1)–(4) are plotted out in Figure 7 for $k_3 = -0{\cdot}005$, and $M_0 = 0{\cdot}3$, $0{\cdot}15$. For $M_0 = 0{\cdot}03$, in the all three resonant regions the smallest amplitudes are obtained for function (4) and the highest ones for functions (1) and (2). When $M_0 = 0{\cdot}15$ this remains true until the assumed function of the moment M_{sp} achieves its maximum. Then, the solution for function (1) diverges to infinity, for function (2) is non-harmonic and the diagrams of the solutions for functions (3) and (4) form the "plateau". That is seen clearly in the first resonant region in Figure 7. The maximum value of the moment for the non-linear spring is equal to $0{\cdot}0608$ for function (1) while $A = 0{\cdot}0645$ for the remaining functions. These values are independent of the number of shafts and the number of rigid bodies in the discrete-continuous model. They are dependent only on assumed parameters k_1, k_3 occurring in the non-linear functions describing the moment M_{sp} (see Figures 3 and 7).

The application ranges of the polynomial function (1) (dashed lines) and the sinusoidal function (2) (continuous lines) are presented in Figure 8 for $k_3 = -0{\cdot}0005$, $-0{\cdot}001$, $-0{\cdot}005$, $-0{\cdot}01$. Similarly, as in the case of the two-mass

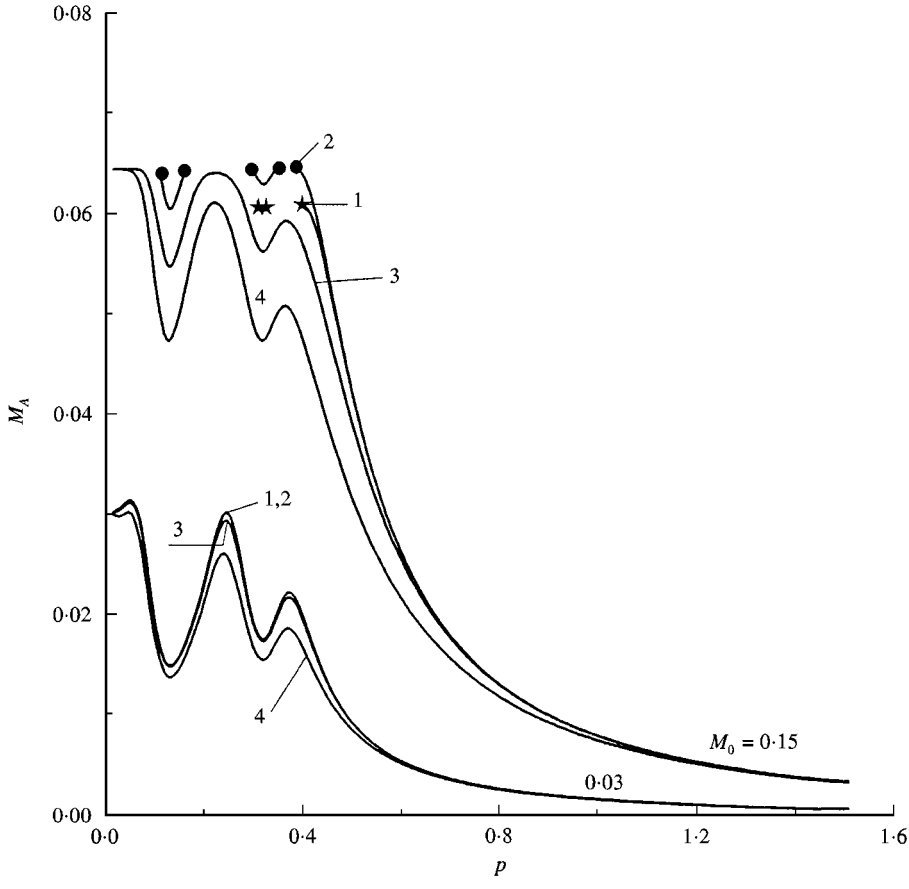

Figure 7. Amplitudes of the moment M_{sp} for the three-mass system for $k_3 = -0{\cdot}005$, $M_0 = 0{\cdot}03$, $0{\cdot}15$ with non-linear functions (1)–(4).

system, the strongest restrictions occur in the neighbourhood of resonances and admissible values of M_0 decrease with the decrease of k_3. For the fixed p the acceptable M_0 is higher for the sinusoidal function. In the case of function (1), between the first and the second resonances there exists the interval of p where these values increase in a linear manner.

The investigations of the effect of various parameters characterizing the discrete-continuous model of torsional systems can be easily performed using functions (3) and (4). For example, in Figure 9 the effect of the parameters k_3, representing the local non-linearity, on displacement amplitudes in $x = 0$ is shown. From Figure 9 it follows that in the case of the three-mass system, in the first and second resonant regions, the maximal amplitudes increase with the decrease of k_3 while in the third resonant region they increase with the increase of k_3.

5. FINAL REMARKS

In this paper it is shown how various non-linear functions can be incorporated in the dynamic analysis of the discrete-continuous models of multi-mass systems

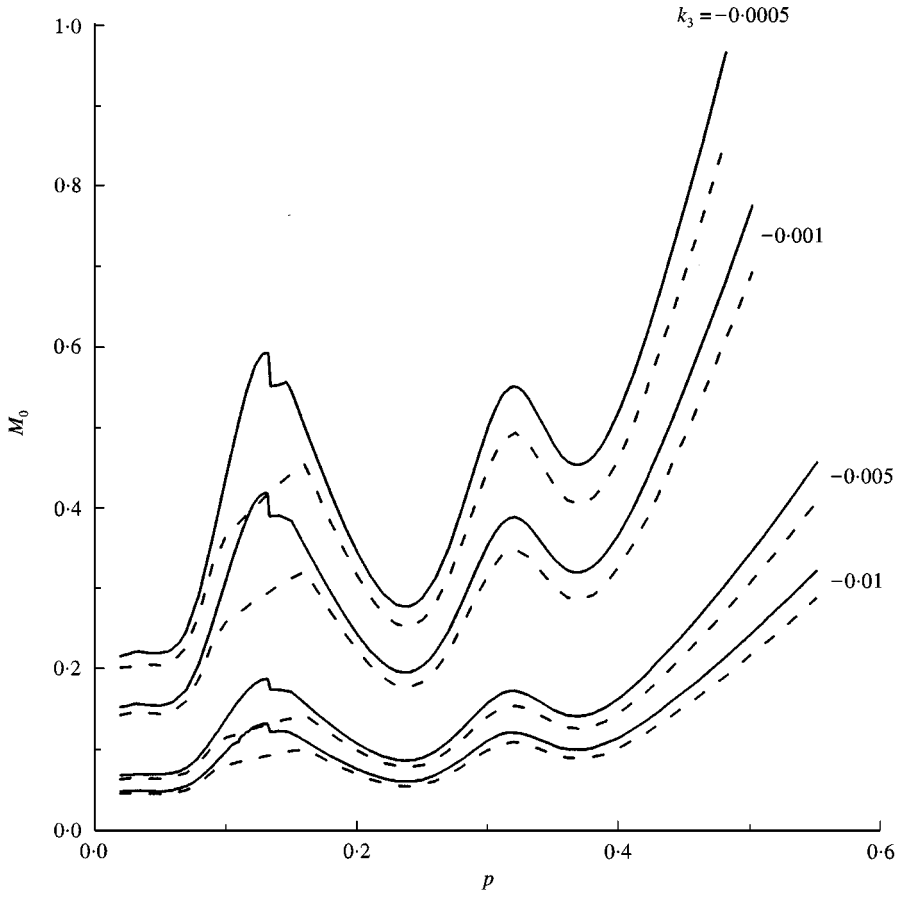

Figure 8. Application ranges of the sinusoidal function (continuous lines) and polynomial function (dashed lines) for the three-mass system with $k_3 = -0{\cdot}0005,\ -0{\cdot}001,\ -0{\cdot}005,\ -0{\cdot}01$.

torsionally deformed having the local non-linearity with the characteristic of a soft type. In the study the third-order polynomial function, the sinusoidal function, the hyperbolic tangent function and the exponential function are proposed for the description of the assumed local non-linearity. It is found that the polynomial and sinusoidal functions have some limits for their application while the last two functions can be applied, when the use of the polynomial and sinusoidal functions leads to solutions losing physical meaning. Within the application ranges of the polynomial function, the solutions for all considered non-linear functions coincide practically.

The numerical calculations are performed for selected parameters describing the two-mass and three-mass torsional systems. Analogous calculations can be executed for systems with other parameters and having more than three rigid bodies. The increase in the number of rigid bodies in the discrete-continuous model of the torsional system will lead to conclusions similar to those given in the present paper. Appropriate diagrams of numerical solutions will include more resonant regions with non-linear effects and will be more complicated.

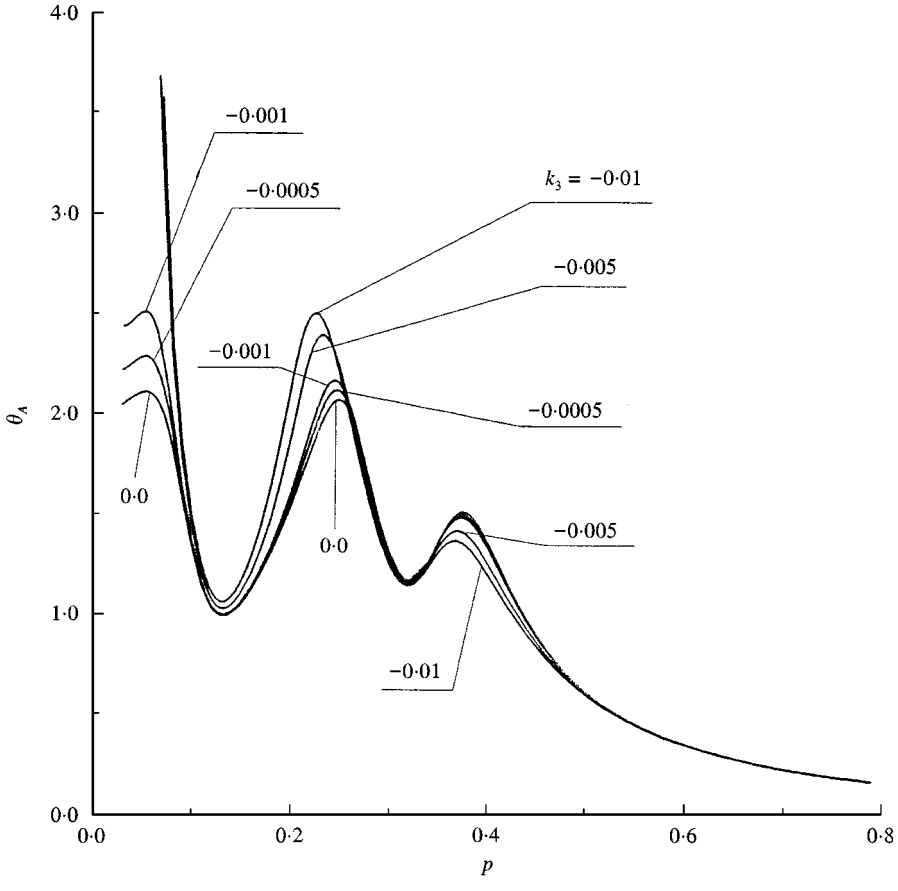

Figure 9. Effect of the parameter k_3 on displacement amplitudes for the three-mass system with $M_0 = 0{\cdot}1$, $k_3 = 0, \ -0{\cdot}0005, \ -0{\cdot}001, \ -0{\cdot}005, \ -0{\cdot}01$ for the hyperbolic tangent function.

REFERENCES

1. A. Pielorz 1995 *Zeitschrift für Angewandte Mathematik und Mechanik* **75,** 691–698. Dynamic analysis of a non-linear discrete-continuous torsional system by means of wave method.
2. W. T. Thomson 1981 *Theory of Vibration with Applications.* Englewood Cliffs, NJ: Prentice-Hall.
3. W. Nadolski 1996 *Meccanica* **31,** 665–672. Influence of nonlinear stiffness of teeth on dynamic loads in gear transmission.
4. Chr. Boiler and T. Seeger 1987 *Materials Data for Cyclic Loading.* Parts A–E, New York: Elsevier.
5. J. M. T. Thompson and S. R. Bishop 1994 *Nonlinearity and Chaos in Engineering Dynamics.* Chichester: Wiley.
6. J. Tödter 1992 *VDI Verlag*, Reihe 11, Nr. 168. Zur Simulation von Drehschwingungen in Antriebssystemen mit lokalen Nichtlinnearitäten.
7. O. Mahrenholtz and T. Szolc 1996 *Dynamical Problems in Mechanical Systems IV* (R. Bogacz, G. P. Ostermeyer and K. Poop editors), 209–220. Poland: Warszawa. Experimental verification of the wave approach for the torsional vibration analysis.

8. R. E. MICKENS 1981 An Introduction to Non-linear Oscillations. Cambridge: Cambridge University Press.
9. P. HAGEDORN 1981 *Non-linear Oscillations*. Oxford: Clarendon Press.
10. W. NADOLSKI, A. PIELORZ and A. MIODUCHOWSKI 1985 *Meccanica* **20,** 164–170. Multi-mass drive system with stepped shafts.